An experimental and theoretical study of the C 1s ionization satellites in CH_3I

Cite as: J. Chem. Phys. 150, 224303 (2019); doi: 10.1063/1.5099699
Submitted: 12 April 2019 • **Accepted:** 17 May 2019 •
Published Online: 11 June 2019

A. B. Trofimov,[1,2] A. M. Belogolova,[1,2] S. A. Serebrennikova,[1] R. Forbes,[3,4,a)] S. T. Pratt,[5] and D. M. P. Holland[6,b)]

AFFILIATIONS

[1] Laboratory of Quantum Chemistry, Irkutsk State University, Karl Marx Str. 1, 664003 Irkutsk, Russia
[2] Favorsky's Institute of Chemistry, SB RAS, Favorsky Str. 1, 664033 Irkutsk, Russia
[3] Department of Physics and Astronomy, University College London, Gower Street, London WC1E 6BT, United Kingdom
[4] Department of Physics, University of Ottawa, 150 Louis Pasteur, Ottawa, Ontario K1N 6N5, Canada
[5] Chemical Sciences and Engineering Division, Argonne National Laboratory, Lemont, Illinois 60439, USA
[6] Daresbury Laboratory, Daresbury, Warrington, Cheshire WA4 4AD, United Kingdom

[a)] **Current address:** PULSE Institute, Stanford Linear Accelerator Centre, Menlo Park, California 94025, USA.
[b)] **Electronic mail:** david.holland@stfc.ac.uk

ABSTRACT

The C 1s ionization spectrum of CH_3I has been studied both experimentally and theoretically. Synchrotron radiation has been employed to record polarization dependent photoelectron spectra at a photon energy of 614 eV. These spectra encompass the main-line due to the C 1s single-hole state and the peaks associated with the shake-up satellites. Vertical ionization energies and relative photoelectron intensities have been computed using the fourth-order algebraic-diagrammatic construction approximation scheme for the one-particle Green's function and the 6-311++G** basis set. The theoretical spectrum derived from these calculations agrees qualitatively with the experimental results, thereby allowing the principal spectral features to be assigned. According to our calculations, two $^2A_1$ shake-up states of the C $1s^{-1}$ $\sigma_{CI} \rightarrow \sigma^*_{CI}$ type with singlet and triplet intermediate coupling of the electron spins ($S' = 0, 1$) play an important role in the spectrum and contribute significantly to the overall intensity. Both of these states are expected to have dissociative diabatic potential energy surfaces with respect to the C–I separation. Whereas the upper of these states perturbs the manifold of Rydberg states, the lower state forms a band which is characterized by a strongly increased width. Our results indicate that the lowest shake-up peak with significant spectral intensity is due to the pair ($S' = 0, 1$) of ^2E (C $1s^{-1}$ I 5p $\rightarrow \sigma^*_{CI}$) states. We predict that these ^2E states acquire photoelectron intensity due to spin-orbit interaction. Such interactions play an important role here due to the involvement of the I 5p orbitals.

I. INTRODUCTION

Core and inner-shell photoelectron spectra of atoms and molecules often display, in addition to the main peak associated with the single-hole state, satellite structure lying at higher binding energies. These satellites, due to shake-up or shake-off processes, correspond to core or inner-shell ionization together with the simultaneous excitation or ionization, respectively, of a valence electron.[1–3] The appearance of such satellites is mainly attributable to correlation effects, due to configuration mixing in the ground and ionized states, and to relaxation effects, due to the readjustment of the orbitals around the core hole.[4] Photoelectron satellites were first observed using monochromated X-ray line sources, for example, Al Kα radiation at ~1487 eV.[1,5] The experimental spectra showed that for K-shell ionization of C, N, or O, ~30% to 40% of the 1s partial photoionization cross section appears in the shake-up and shake-off satellites.

Subsequent studies using synchrotron radiation, mainly on molecules composed of low atomic number atoms, have enabled the shake-up satellites to be investigated in greater detail (e.g.,

Refs. 6–11). In these experiments, polarization dependent photoelectron spectra were recorded using both high photon resolution and high electron kinetic energy resolution, thereby allowing the anisotropy parameter which characterizes the angular distribution to be determined. Moreover, spectra were measured over an extended photon energy range so that the variation in the satellite cross section could be examined. Such dynamical information helps assign the electronic symmetry of the satellite state and may reveal the processes leading to the satellite formation. In the most recent experimental studies,[12–16] the overall resolution has been sufficient to enable the vibrational structure associated with a particular satellite, and the polarization dependence of this structure, to be observed. A comparison between the experimental spectra and the predicted vibrational population distributions allowed the geometry of the excited state to be determined.

Satellite states are generally classified into two categories,[2,3,17–20] according to whether their intensity arises from the so-called direct or conjugate contributions (see also the Appendix). In the direct shake-up process, the dipole ionization of a core electron is accompanied by the monopole excitation of one or more valence electrons. This contribution dominates the spectral intensity at high electron energies (in the sudden limit[21]) but becomes less important as the photon energy approaches threshold. In the conjugate shake-up process, the monopole ionization of a core electron is accompanied by the dipole excitation of valence electrons. The conjugate contribution may be significant at low electron energies, but at high energy it becomes negligible since the overlap integrals decrease rapidly with increasing energy. The selection rules for both the direct and the conjugate processes require the overall (electron plus ion) wave function symmetry to be the same as the symmetry of at least one component of the dipole operator. However, in the direct process, the ion wave function has the same symmetry as the main-line process, while, in the conjugate process, the electron wave function has the same symmetry as the main-line process (see the Appendix). Thus, the conjugate process allows satellite states having electronic symmetries that are forbidden in the direct process to appear near threshold.

Our experimental and theoretical study concerns the photoelectron satellites associated with the C 1s ionization spectrum of methyl iodide (Fig. 1) and differs from previous investigations in that the molecule contains an atom (iodine) of high atomic number. This raises the interesting question of whether spin-orbit interactions play a role in the formation of the satellites. Our experimental spectrum exhibits a shake-up satellite lying at a binding energy ~3 eV higher than that of the peak due to the C $1s^{-1}$ single-hole state. This satellite, according to our calculations, arises from C K-shell ionization accompanied by a transition from the outermost valence orbital into the lowest lying vacant molecular orbital (MO). The energy separation between this satellite and the main-line is unusually small. The first shake-up satellite in the C 1s photoelectron spectrum of the closely related methane (CH_4) molecule is located ~17 eV above the main-line.[6] Indeed, the energy separation of ~3 eV between the lowest energy satellite and the main-line in CH_3I is smaller than that observed in the C K-shell photoelectron spectrum of several hydrocarbon molecules.[7–11] In some respects our results for the C 1s spectrum of CH_3I are similar to those for the corresponding C 1s spectrum of CO, which has been studied extensively, both experimentally[15,16,22–28] and theoretically.[29–36]

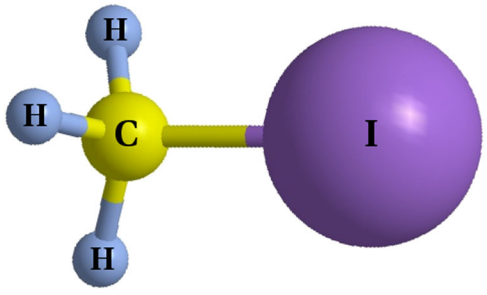

FIG. 1. Schematic representation of CH_3I.

We have employed the fourth-order algebraic-diagrammatic construction [ADC(4)] approximation scheme for the one-particle Green's function[37,38] to calculate the vertical ionization energies and the relative photoelectron intensities of the C 1s ionization spectrum of CH_3I. These theoretical predictions have been used to interpret the structure observed in the corresponding photoelectron spectrum recorded with synchrotron radiation. Our study leads to the conclusion that spin-orbit interactions need to be taken into account to explain the appearance of some of the satellite structure.

II. EXPERIMENTAL APPARATUS AND PROCEDURE

The experiments were carried out on the soft X-ray undulator-based PLÉIADES beamline at the SOLEIL synchrotron radiation facility. Detailed descriptions of the beamline and station instrumentation have been reported previously[39–41] so only a summary is given here.

Plane polarized synchrotron radiation, derived from an Apple II type undulator, was monochromated with a plane grating, modified-Petersen type monochromator and delivered into the interaction region of a VG Scienta R4000 electron analyzer. The degree of polarization was determined to be >99%.[40] The plane of polarization could be rotated through 90°, thereby allowing photoelectron angular distributions to be measured with the electron analyzer in a fixed position.

Photoelectron spectra were recorded with the plane of polarization set either parallel or perpendicular to the direction of the electron's path toward the detector using a monochromator exit slit width of 70 μm, together with an electron spectrometer entrance slit width of 0.5 mm and a pass energy of 50 eV. These settings result in theoretical photon and electron spectrometer resolutions of ~300 and ~60 meV, respectively. A higher resolution spectrum was recorded with the plane of polarization set parallel to the electron's path, using a monochromator slit width of 20 μm, together with an electron analyzer slit width of 0.6 mm and a pass energy of 50 eV. Using these settings, the resulting theoretical photon and electron spectrometer resolutions are both ~100 meV.

Translational Doppler broadening, associated with the thermal motion of the room temperature CH_3I sample molecules, contributes to the photoelectron peak width.[42] At a photon energy

of 614 eV, this broadening amounts to ~19 meV for the C 1s main-line.

The transmission efficiency of the electron analyzer was determined as described by Jauhiainen *et al.*[43] The electron binding energy scale was calibrated using the C 1s in CH_3I ionization energy given by Hitchcock and Brion.[44]

III. COMPUTATIONAL DETAILS

The reliable theoretical treatment of the satellite states in core ionization spectra is an extremely challenging task in view of the strong electron correlation and orbital relaxation effects that accompany the formation of such states. High-level quantum chemistry electronic structure methods,[33–38] therefore, have to be used in such calculations. In the present work, the vertical transition energies and the relative photoelectron intensities (pole strengths) in the C 1s ionization spectrum of CH_3I were computed using the ADC(4) approximation scheme for the one-particle Green's function.[37,38] In addition, our calculations employed the core-valence separation (CVS) approximation[45] which considerably simplifies the theoretical scheme and reduces the computational effort. This approximation is based on the fact that the core and valence-shell ionized states are separated by extremely large energy gaps and the corresponding wavefunctions have negligible overlap with each other. In the ADC(4)/CVS method, the final cationic states are described in terms of the one-hole (1h), two-hole-one-particle (2h-1p), and three-hole-two-particle (3h-2p) configurations which are treated through fourth, second, and first order of the many-body perturbation theory, respectively. More precisely, the ADC(4) variant being used can be referred to as an "extended" ADC(4) method since, as stated above, the coupling between the 3h-2p configurations is treated through first-order, whereas in the "strict" ADC(4) scheme only their zero-order treatment is required.[37] Such an extension improves the results for the 2h-1p shake-up satellite states in those cases where the satellites include a considerable 3h-2p character, as well as improving the results for the 3h-2p satellite states. As a consequence of the CVS approximation, the configurational space is restricted to the configurations possessing exactly one C 1s hole. Hence, only the lowest eigenvalues and eigenvectors of the ADC(4)/CVS secular matrix are required to obtain a description of the C 1s ionization spectrum.[30]

In the ADC(4) approach, all the main effects accompanying ionization, such as electron correlation in the initial and final states and orbital relaxation, are taken into account in a consistent manner. This ensures a reliable description of most of the types of final states accessible by photoelectron spectroscopy. Such states include the single-hole states, various shake-up satellites, and the states characterized by a strong mixing between the 1h and 2h-1p configurations, responsible for the phenomenon known as the break-down of the one-electron picture of ionization.[4] These are prerequisites for adequate theoretical studies of core-level photoelectron shake-up spectra. Moreover, the huge relaxation energy associated with the formation of the core-hole states can be satisfactorily accounted for only in electronic structure methods treating such processes at least through fourth-order.[29,30] The ADC(4)/CVS method[30] has been shown to provide a very satisfactory treatment of various core level ionization phenomena,[46–51] and it appears to be ideally suited to the present study of the C 1s shake-up satellites in CH_3I.

TABLE I. Calculated [MP2/6-311++G**(A)] and experimental equilibrium geometrical parameters of CH_3I (bond lengths in Å and angles in degrees) in the neutral ground state (X^1A_1).

Parameter	MP2, this work	Expt.[a]
	Bond length	
C–I	2.146	2.136
C–H	1.087	1.084
	Angle	
H–C–I	108.0	107.5

[a]Reference 59.

The ADC(4)/CVS calculations were performed using the original code[52] linked to the Gamess *ab initio* program package.[53,54] The theoretical spectral profiles were constructed by convoluting the ADC(4) spectrum with Gaussians of 0.5 eV FWHM (full width at half maximum).

The ground-state characteristics of CH_3I were computed using the 6-311++G** basis set[55,56] on the carbon and hydrogen atoms and the 6-311G** basis set[57] on the iodine atom. The resulting basis is henceforth denoted as 6-311++G**(A). The ADC(4) calculations were performed using the 6-311++G**(B) basis set, which was obtained from the 6-311++G**(A) basis by augmenting the basis on the iodine by a set of diffuse functions with the following exponents: 0.037 (s), 0.014 (s), 0.032 (p), 0.012 (p), 0.08 (d), and 0.02 (d), obtained in the even-tempered manner with respect to the two smallest exponents of each symmetry of the standard 6-311G** basis set.[57] The Cartesian representation of the d-functions was adopted in the calculations.

The ground-state geometrical parameters were obtained by means of the full geometry optimization at the level of the second-order Møller-Plesset perturbation theory (MP2), which was carried out using the Gaussian package of programs.[58] The results obtained in this procedure (Table I) agree well with the experimental data,[59] thus confirming the theoretical consistency of our modeling. More specifically, our calculations accurately reproduce the C–H bond lengths and the H–C–I angle but somewhat overestimate the C–I bond length.

IV. RESULTS AND DISCUSSION

A. Valence-shell orbital structure of CH_3I

According to our Hartree-Fock (HF) calculations, the ground-state electronic configuration of CH_3I (C_{3v} point group symmetry) is

$$1a_1(C\,1s)^2\,2a_1(I4s)^2\,3a_1(I4p)^2\,1e(I4p)^4\,4a_1(I4d)^2\,2e(I\,4d)^4\,3e(I\,4d)^4$$
$$5a_1(\sigma_{CH})^2\,6a_1(\sigma_{I\,5s})^2\,4e(\sigma_{CH})^4\,7a_1(\sigma_{CI})^2\,5e(I\,5p)^4.$$

The deeper molecular orbitals (MOs) representing the 1s, 2s, 2p, 3s, 3p, and 3d atomic orbitals (AOs) of iodine were excluded from the

TABLE II. Mulliken atomic population in the outer-valence shells of CH_3I calculated at the HF/6-311++G**(A) level of theory (units are electrons; sum over all atoms equals two for each occupied orbital; for the unoccupied shells, $12a_1$, 9e, and $13a_1$, the results were obtained by formally assuming the sum over all atoms to be equal to one for each unoccupied orbital; see text for details).

Atom	$5a_1$ (σ_{CH})	$6a_1$ ($\sigma_{I\,5s}$)	4e (σ_{CH})	$7a_1$ (σ_{CI})	5e (I 5p)	$12a_1$ (σ^*_{CI})	9e (σ^*_{CH})	$13a_1$ (σ^*_{CH})
I	0.11	1.57	0.12	1.13	3.89	0.61	−0.28	−0.24
C	1.48	0.27	2.19	0.75	0.02	−1.83	−1.90	−1.11
H	0.14	0.05	0.56	0.04	0.03	0.74	1.39	0.79

present numbering scheme. All these orbitals, as well as those representing the iodine 4s, 4p, and 4d AOs, were kept frozen in our ADC(4) calculations. The orbital assignment shown in parentheses is to a large extent supported by the Mulliken atomic populations[60] given in Table II.

The orbital structure of CH_3I can also be understood very well from the following qualitative considerations. Three of the four sp^3 hybrid AOs of carbon interact with the three hydrogen 1s AOs to form three σ_{CH} bonding and three antibonding σ^*_{CH} MOs. The remaining sp^3 AO of carbon, 5s and one of the iodine 5p AOs form σ^*_{CI} and σ^*_{CH} bonding and antibonding orbitals. The two 5p AOs of iodine not involved in these interactions remain largely intact and represent nonbonding (n) MOs, also referred to as iodine lone-pairs (LPs). The σ_{CH} orbitals can be identified readily as the $5a_1$ and 4e MOs (Table II), while the σ_{CI} orbital can be identified as the $7a_1$ MO. Further inspection of the data in Table II and the calculated MOs allows the I 5p AOs to be assigned to the 5e MOs. The $6a_1$ MO retains significant I 5s character and can, therefore, be referred to as a $\sigma_{I\,5s}$ orbital.

The unoccupied MOs are more difficult to assign since they were obtained in our calculations using a basis set with diffuse functions and, hence, often have a mixed valence-Rydberg character. Moreover, complications arise because the iodine AOs have a complex nodal structure. To obtain a reasonable interpretation of the character of the unoccupied MOs, we use a procedure analogous to the Mulliken population analysis in which we formally set the occupation numbers of these orbitals to one. The resulting quantities—although being not strictly physically defined—allow the localization properties of the unoccupied MOs to be understood (Table II). As follows from such an analysis, the σ^*_{CI} orbital is rather well represented by the $12a_1$ MO, and the σ^*_{CH} orbitals, to a good approximation, can be identified as the 9e and $13a_1$ MOs. The remaining unoccupied orbitals have Rydberg or mixed valence-Rydberg character with predominant iodine localization.

B. Overview of the experimental C 1s satellite spectrum

Figure 2 shows photoelectron spectra encompassing the C 1s single-hole state and the shake-up satellites recorded with parallel or perpendicular plane of polarization geometries. The photoelectron anisotropy parameter (β) characterizing the angular distribution can be derived from such spectra.[39] However, as the electron

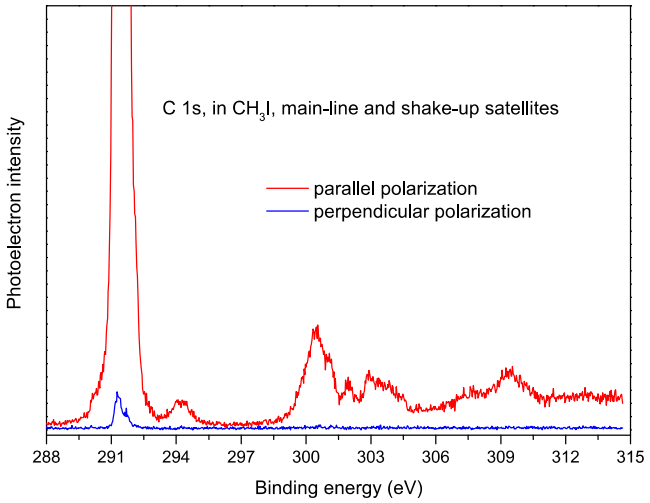

FIG. 2. Photoelectron spectra of CH_3I recorded at a photon energy of 614 eV, with the plane of polarization lying parallel (red) or perpendicular (blue) to the direction of the electron's path toward the detector. These spectra were measured using a monochromator exit slit width of 70 μm, together with an electron spectrometer entrance slit width of 0.5 mm and a pass energy of 50 eV. The binding energy range encompasses the peaks due to the C $1s^{-1}$ main-line and the shake-up satellites.

intensity in the spectrum recorded with the plane of polarization in the perpendicular orientation is negligible, apart from a very small contribution in the peak associated with the single-hole state, the β parameter is ~2 (its maximum value) across the entire spectrum.

Our photoelectron spectra were recorded at a photon energy well above the C 1s ionization threshold. Hence, only the direct shake-up process should contribute significantly to the satellite intensity. In this limit, the energy dependence of the anisotropy parameter associated with a satellite state should resemble that of the main-line state.[15] Previous experimental studies on the C 1s shake-up satellites in ethane,[8] benzene,[10] and carbon monoxide[28] have confirmed this prediction, with the β-parameter for the single-hole state and those for the satellite states exhibiting a high value at photon energies well above threshold. Thus, the present observation that the β-parameter for the C 1s main-line and those for the satellite peaks of CH_3I all possess a similar high value is consistent with the expectation that only the direct shake-up process contributes intensity to the satellites in our spectrum recorded at a photon energy of 614 eV.

C. Interpretation of the C 1s shake-up spectrum based on the theoretical results

The C 1s ionization spectrum of CH_3I comprises the main (single-hole) C $1s^{-1}$ ionization line and the ionization satellites. The satellites appearing at low binding energies (~293–303 eV) are represented mainly by states of 2h-1p character, but at higher energy, states of 3h-2p character also contribute. These groups of satellites can be viewed as single and double valence-shell electron excitations, respectively, of the C $1s^{-1}$ cation. The 2h-1p states can be

TABLE III. Symmetry of possible excited states of neutral and C 1s-ionized CH_3I obtained by an electron excitation from the highest occupied orbitals into unoccupied orbitals of valence and Rydberg type. For the neutral, each state occurs with the total spin $S = 0, 1$. In the C $1s^{-1}$ cation, the possible total spin values are $S = 1/2$ (two independent spin states, corresponding to the intermediate coupling of two electrons $S' = 0, 1$) and $S = 3/2$.

Unoccupied MOs (type and symmetry)		4e (σ_{CH}) → 5e (I 5p) →	6a$_1$ ($\sigma_{I\,5s}$) → 7a$_1$ (σ_{CI}) →
		Valence	
σ^*_{CI}	a_1	E	A_1
σ^*_{CH}	e	A_1, E, A_2	E
	a_1	E	A_1
		Rydberg	
ns	a_1	E	A_1
np	a_1	E	A_1
	e	A_1, E, A_2	E
nd	a_1	E	A_1
	e	A_1, E, A_2	E
	e	A_1, E, A_2	E

characterized further, according to the type of orbital involved, as valence or Rydberg type excitations (Table III).

In this work, we denote the Rydberg series due to the excitation of an electron from the 5e, 7a$_1$, 4e, . . . molecular orbitals as R, R′, R″, . . ., respectively. As can be seen from Table III, each series comprises electronic states of A_1, E, and A_2 symmetry resulting from the splitting of the spherically symmetric atomic orbitals by the molecular field.

To discuss the 2h-1p core-hole ionization satellites in more detail, we adopt the accepted view[29,30,32] that the singlet and triplet excited states ($S' = 0,1$) couple to the core electron and yield two doublet states ($S = 1/2$) and one quartet state ($S = 3/2$) for each of the spatial symmetry species.[29] In this picture, the two doublet states correspond to the $S' = 0,1$ intermediate coupling of the valence electrons, although two further coupling schemes of the three electrons are possible.[29,30,32] The intermediate spin S' is not a conserved quantity, so the exact and the ADC(4) eigenstates correspond to linear combinations of these basis states rather than to the pure states in any of the three coupling schemes. However, the scheme with the intermediate coupling of the valence electrons, just described, plays a somewhat privileged role as it is characterized by the smallest Hamiltonian matrix element between the two doublets, thus providing the best zero-order approximation for the final core-ionized 2h-1p states.[29,30,32] Here we also note that all our calculations were performed using a nonrelativistic *ab initio* approach, and no attempt has been made to treat the spin-orbit coupling effects associated with the iodine atom. The present theoretical study has, therefore, only a preliminary character, and the discussion of the spectroscopic implications of spin-orbit coupling is postponed to our forthcoming publications.

Table IV contains a partial listing of the results of our ADC(4) calculations. All the predicted satellite states having binding energies below 304 eV are given in Table IV, but for higher binding energies only those states of $^2A_1$ symmetry are listed. A complete summary of all the predicted satellites is given in Table S1 of the supplementary material. The theoretical spectrum obtained from our ADC(4) results is shown in Fig. 3, together with the higher resolution (see Sec. II for details) experimental data. The assignments of the satellite states were made according to the type of the formally largest configuration in the expansion of the ADC(4) eigenvectors, taking into account the information provided in Tables II and III. In most cases, a very strong configuration mixing was obtained, with many comparable contributions of relatively small magnitude. The present assignments are, therefore, only very qualitative, and many states in fact have a more complex mixed character. In particular, and probably for this reason, no individual members of the Rydberg series could be assigned using the familiar approach based on the perturbed Rydberg formula fitting.

The calculated vertical ionization energy (291.18 eV) for the C 1s main-line, which corresponds to the 1^2A_1 (C $1s^{-1}$) state of CH_3I, is in excellent agreement with the measured value (291.3 eV[44]). However, it should be noted that for a stringent comparison with experiment, a relativistic correction of about +0.1 eV and a correction of −0.4 eV for the core-valence separation should be applied to the calculated ionization energy.[30] Nevertheless, the corrected theoretical value (290.88 eV) is still very close to the experimental measurement. The absolute pole strength for the main state is 0.59, which means that about 40% of the C 1s photoionization partial cross section appears in the satellites.

Our calculations predict that the lowest shake-up transitions in the spectrum [denoted as A_1 and A_2 in Fig. 3(b)] are due to the pair of closely spaced (1,2) ^{2}E (C $1s^{-1}$ I 5p → σ^*_{CI}) states differing by the intermediate spin coupling. The calculated vertical binding energy of the lower $S' = 1$ state is 293.88 eV, whereas that of the higher-lying $S' = 0$ state is 295.0 eV. The average of these two ionization energies (294.44 eV) agrees very well with the energy of the first satellite peak, at 294.3 eV, in the experimental spectrum. The excitation of an electron from the nonbonding I 5p orbital to the σ^*_{CI} valence orbital, with predominant carbon localization (Table II), leads to an efficient screening of the C 1s hole.[30] This screening accounts for the location of the ^{2}E states at very low binding energies.

The substantial intensity in the experimental band under consideration, however, cannot be understood within the present nonrelativistic framework. As is well known,[17,18,29] the monopole selection rules (emerging from the expression for the dominant direct part of the photoelectron intensity) do not allow satellite states having symmetry other than the symmetry of the main $^2A_1$ state to acquire intensity in the C 1s ionization spectrum of CH_3I (see the Appendix). The symmetry selection rules applicable to our calculations, therefore, result in zero intensity being predicted for transitions to the (1,2) ^{2}E (C $1s^{-1}$ I 5p → σ^*_{CI}) states.

To understand the processes leading to the satellite formation and the energy dependence of these mechanisms, we consider the direct and conjugate contributions to the intensity of the 1^2E ($1a_1^{-1}$ $5e^{-1}$ $12a_1$) satellite state. In zero order of the perturbation theory, neglecting the construction of the wavefunctions with

TABLE IV. Binding energies E (eV) and relative photoelectron intensities P (in percent with respect to the pole strength of the C $1s^{-1}$ main-line) of the C 1s vertical ionization transitions in CH_3I up to 20 eV relative to the C $1s^{-1}$ main line, computed using the ADC(4) method and the 6-311++G** (B) basis set.[a]

State	Configuration[b]	S'[c]	Assignment[d]	E	P	Expt.[e]
$1\,^2A_1$	$1a_1^{-1}$		C $1s^{-1}$	291.18	100.0[f]	291.28
$1\,^2E$	$1a_1^{-1}\ 5e^{-1}\ 12a_1$	1	I 5p-σ^*_{CI} (A_1)	293.88	...	294.27
$2\,^2E$	$1a_1^{-1}\ 5e^{-1}\ 12a_1$	0	I 5p-σ^*_{CI} (A_2)	295.00	...	294.27
$3\,^2E$	$1a_1^{-1}\ 5e^{-1}\ 13a_1$	1	I 5p-σ^*_{CH}	298.90	...	
$2\,^2A_1$	$1a_1^{-1}\ 7a_1^{-1}\ 12a_1$	1	σ_{CI}-σ^*_{CI} (B_1)	299.09	0.8074	297.6–297.8
$4\,^2E$	$1a_1^{-1}\ 5e^{-1}\ 13a_1$	0	I 5p-σ^*_{CH}	299.31	...	297.6–297.8
$3\,^2A_1$	$1a_1^{-1}\ 5e^{-1}\ 9e$	1	I 5p-σ^*_{CH} (B_2)	300.15	0.0493	
$5\,^2E$	$1a_1^{-1}\ 5e^{-1}\ 9e$	1	I 5p-σ^*_{CH}	300.23	...	
$1\,^2A_2$	$1a_1^{-1}\ 5e^{-1}\ 9e$	1	I 5p-σ^*_{CH}	300.26	...	
$4\,^2A_1$	$1a_1^{-1}\ 5e^{-1}\ 9e$	0	I 5p-σ^*_{CH} (B_2)	300.43	0.0003	
$6\,^2E$	$1a_1^{-1}\ 5e^{-1}\ 9e$	0	I 5p-σ^*_{CH}	300.52	...	
$2\,^2A_2$	$1a_1^{-1}\ 5e^{-1}\ 9e$	0	I 5p-σ^*_{CH}	300.54	...	
$5\,^2A_1$	$1a_1^{-1}\ 5e^{-1}\ 11e$	1	R (C_1)	300.90	0.0051	
$7\,^2E$	$1a_1^{-1}\ 5e^{-1}\ 14a_1$	1	R	301.02	...	
$6\,^2A_1$	$1a_1^{-1}\ 7a_1^{-1}\ 12a_1$	0	σ_{CI}-σ^*_{CI} (C_1)	301.10	3.2429	300.50
$8\,^2E$	$1a_1^{-1}\ 5e^{-1}\ 14a_1$	1	R	301.22	...	
$3\,^2A_2$	$1a_1^{-1}\ 5e^{-1}\ 11e$	1	R	301.30	...	
$7\,^2A_1$	$1a_1^{-1}\ 5e^{-1}\ 13e$	1	R (C_1)	301.32	0.1567	
$9\,^2E$	$1a_1^{-1}\ 5e^{-1}\ 14a_1$	0	R	301.35	...	
$4\,^2A_2$	$1a_1^{-1}\ 5e^{-1}\ 11e$	0	R	301.43	...	
$10\,^2E$	$1a_1^{-1}\ 5e^{-1}\ 11e$	0	R	301.54	...	
$11\,^2E$	$1a_1^{-1}\ 5e^{-1}\ 13e$	1	R	301.74	...	
$8\,^2A_1$	$1a_1^{-1}\ 7a_1^{-1}\ 12a_1$	0	σ_{CI}-σ^*_{CI}/R′ (C_2)	301.83	2.0048	301.13
$5\,^2A_2$	$1a_1^{-1}\ 5e^{-1}\ 13e$	1	R	302.11	...	
$6\,^2A_2$	$1a_1^{-1}\ 5e^{-1}\ 13e$	0	R	302.24	...	
$12\,^2E$	$1a_1^{-1}\ 5e^{-1}\ 15a_1$	1	R	302.24	...	
$9\,^2A_1$	$1a_1^{-1}\ 5e^{-1}\ 10e$	1	R (C_2)	302.31	0.0213	
$7\,^2A_2$	$1a_1^{-1}\ 5e^{-1}\ 13e$	0	R	302.32	...	
$10\,^2A_1$	$1a_1^{-1}\ 5e^{-1}\ 13e$	0	R (C_2)	302.32	<0.0001	
$13\,^2E$	$1a_1^{-1}\ 5e^{-1}\ 15a_1$	0	R	302.35	...	
$8\,^2A_2$	$1a_1^{-1}\ 5e^{-1}\ 10e$	1	R	302.54	...	
$11\,^2A_1$	$1a_1^{-1}\ 5e^{-1}\ 10e$	1	R (C_2)	302.54	<0.0001	
$9\,^2A_2$	$1a_1^{-1}\ 5e^{-1}\ 10e$	1	R	302.68	...	
$10\,^2A_2$	$1a_1^{-1}\ 5e^{-1}\ 10e$	0	R	302.81	...	
$12\,^2A_1$	$1a_1^{-1}\ 5e^{-1}\ 6e$	0	R (D)	302.95	0.9333	
$14\,^2E$	$1a_1^{-1}\ 5e^{-1}\ 8e$	0	R	302.98	...	
$15\,^2E$	$1a_1^{-1}\ 5e^{-1}\ 8a_1$	1	R	303.14	...	
$13\,^2A_1$	$1a_1^{-1}\ 5e^{-1}\ 7e$	0	R (D)	303.32	1.6406	301.97
$16\,^2E$	$1a_1^{-1}\ 5e^{-1}\ 8a_1$	0	R	303.36	...	
$11\,^2A_2$	$1a_1^{-1}\ 5e^{-2}\ 12a_1\ 14a_1$	1	R	303.53	...	
$14\,^2A_1$	$1a_1^{-1}\ 5e^{-1}\ 14e$	1	R (D)	303.73	0.0037	
$17\,^2E$	$1a_1^{-1}\ 5e^{-1}\ 13e$	1	R	303.87	...	

TABLE IV. (*Continued.*)

State	Configuration[b]	S'[c]	Assignment[d]	E	P	Expt.[e]
For higher binding energies, only states of $^2A_1$ symmetry are listed[a]						
15 $^2A_1$	$1a_1^{-1}$ $5e^{-1}$ 6e	1	R (E_1)	304.11	0.0132	
16 $^2A_1$	$1a_1^{-1}$ $5e^{-1}$ 8e	1	R (E_1)	304.24	0.0020	
17 $^2A_1$	$1a_1^{-1}$ $7a_1^{-1}$ $13a_1$	0	σ_{CI}-σ^*_{CH} (E_1)	304.29	0.1420	
18 $^2A_1$	$1a_1^{-1}$ $5e^{-1}$ 12e	0	R (E_1)	304.33	0.0115	
19 $^2A_1$	$1a_1^{-1}$ $5e^{-1}$ 8e	0	R (E_1)	304.43	0.0756	
20 $^2A_1$	$1a_1^{-1}$ $7a_1^{-1}$ $13a_1$	1	σ_{CI}-σ^*_{CH} (E_1)	304.55	0.1356	
21 $^2A_1$	$1a_1^{-1}$ $4e^{-1}$ $12a_1$	0	σ_{CH}-σ^*_{CI} (E_1)	304.69	<0.0001	
22 $^2A_1$	$1a_1^{-1}$ $5e^{-1}$ 7e	1	R (E_1)	304.70	0.0453	
23 $^2A_1$	$1a_1^{-1}$ $5e^{-1}$ 7e	1	R (E_1)	304.75	0.1794	
24 $^2A_1$	$1a_1^{-1}$ $5e^{-1}$ 10e	0	R (E_2)	304.98	1.9277	302.87–304.50
25 $^2A_1$	$1a_1^{-1}$ $5e^{-1}$ 9e	1	R (E_2)	305.25	0.2366	302.87–304.50
26 $^2A_1$	$1a_1^{-1}$ $5e^{-1}$ 9e	1	R (E_2)	305.41	0.1299	
27 $^2A_1$	$1a_1^{-1}$ $6a_1^{-1}$ $12a_1$	1	$\sigma_{I\,5s}$-σ^*_{CI} (E_2)	305.48	0.0004	
28 $^2A_1$	$1a_1^{-1}$ $5e^{-1}$ 13e	0	R (E_2)	305.62	1.1968	
29 $^2A_1$	$1a_1^{-1}$ $7a_1^{-1}$ $14a_1$	0	R′ (F)	306.70	0.0964	
30 $^2A_1$	$1a_1^{-1}$ $6a_1^{-1}$ $12a_1$	0	$\sigma_{I\,5s}$-σ^*_{CI} (F)	307.11	0.0131	
31 $^2A_1$	$1a_1^{-1}$ $7a_1^{-1}$ $14a_1$	1	R′ (F)	307.24	0.4090	305.6
32 $^2A_1$	$1a_1^{-1}$ $4e^{-1}$ 14e	1	σ_{CH}-σ^*_{CH} (F)	307.54	0.1844	
33 $^2A_1$	$1a_1^{-1}$ $7a_1^{-1}$ $15a_1$	0	R′ (F)	307.82	0.0266	
34 $^2A_1$	$1a_1^{-1}$ $7a_1^{-1}$ $15a_1$	1	R′ (F)	308.44	0.0013	
35 $^2A_1$	$1a_1^{-1}$ $7a_1^{-1}$ $8a_1$	0	R′ (F)	308.77	0.0034	
36 $^2A_1$	$1a_1^{-1}$ $5e^{-1}$ 15e	1	R (G_1)	308.99	0.0001	
37 $^2A_1$	$1a_1^{-1}$ $7a_1^{-1}$ $8a_1$	1	R′ (G_1)	309.33	0.0003	
38 $^2A_1$	$1a_1^{-1}$ $7a_1^{-1}$ $16a_1$	0	R′ (G_1)	309.63	0.0482	307.7
39 $^2A_1$	$1a_1^{-1}$ $7a_1^{-1}$ $9a_1$	0	R′ (G_1)	309.98	0.0200	
40 $^2A_1$	$1a_1^{-1}$ $7a_1^{-1}$ $16a_1$	1	R′ (G_1)	310.29	0.0485	
41 $^2A_1$	$1a_1^{-1}$ $7a_1^{-1}$ $8a_1$	1	R′ (G_1)	310.40	0.0011	
42 $^2A_1$	$1a_1^{-1}$ $7a_1^{-1}$ $11a_1$	0	R′ (G_1)	310.52	0.0242	
43 $^2A_1$	$1a_1^{-1}$ $6a_1^{-1}$ $13a_1$	0	$\sigma_{I\,5s}$-σ^*_{CH} (G_2)	310.71	0.0253	309.4
44 $^2A_1$	$1a_1^{-1}$ $7a_1^{-1}$ $9a_1$	1	R′ (G_2)	310.77	0.0444	
45 $^2A_1$	$1a_1^{-1}$ $5e^{-1}$ 16e	1	R	310.91	<0.0001	
46 $^2A_1$	$1a_1^{-1}$ $7a_1^{-1}$ $10a_1$	0	R′ (G_2)	311.02	0.0349	
47 $^2A_1$	$1a_1^{-1}$ $5e^{-1}$ 16e	0	R (G_2)	311.12	1.4973	

[a] All the predicted satellite states having binding energies below 304 eV are given. For higher binding energies, only those states of $^2A_1$ symmetry are listed. A complete summary of all the predicted satellites is given in the supplementary material.
[b] Configuration with the (formally) largest weight.
[c] Intermediate spin S' characterizing coupling between the two electrons in the valence orbitals of the specified configuration with the largest weight; further coupling to the core-hole electron yields final states with $S = 1/2$.
[d] Qualitative interpretation of a transition and spectral maximum to which it contributes [Fig. 3(b)]; the common C $1s^{-1}$ part of the shake-up electron configurations is not shown.
[e] Peak maximum or an energy range for the spectral feature in the experimental spectrum [Fig. 3(a)].
[f] Absolute pole strength $P_{abs} = 0.5913$ (see text for details).

correct spatial and spin symmetry, the 1^2E state can be approximated by the single HF determinant $|\Phi^{N-1}_{aij}\rangle = |12a_1\ 5e\ 1a_1\rangle$. Then Eqs. (A13) and (A14) of the Appendix can be used to analyze the direct and conjugate parts of the transition dipole moment, $D(\mathrm{I})$ and $D(\mathrm{II})$, respectively. According to Eq. (A13), the direct part vanishes for all 2h-1p final states [$D(\mathrm{I}) = 0$]. The conjugate part for the ionization into the εa_1 continuum may be expressed as

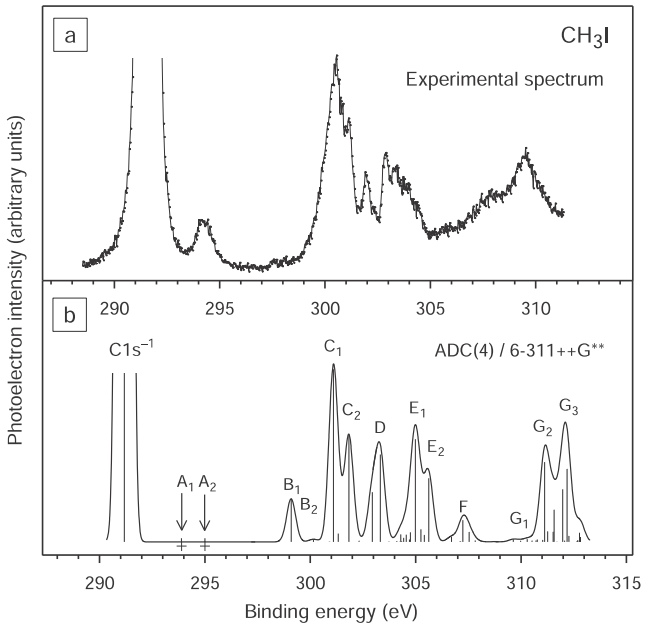

FIG. 3. Experimental (a) and theoretical (b) C 1s ionization spectra of CH_3I. The experimental spectrum was measured using a monochromator exit slit width of 20 μm, together with an electron spectrometer entrance slit width of 0.6 mm and a pass energy of 50 eV. The experimental and theoretical spectra are aligned with respect to the position of the most intense satellite band (the band in the experimental spectrum with the maximum at 300.5 eV). This introduces an overall shift of 0.7 eV, to lower energy, to the theoretical spectrum.

$$D(\mathrm{II}) = \langle 1a_1 | \varepsilon a_1 \rangle \langle 5e | \hat{d} | 12a_1 \rangle \delta_{1a_1,1a_1},$$

and for the ionization into the εe continuum as

$$D(\mathrm{II}) = \langle 1a_1 | \varepsilon e \rangle \langle 5e | \hat{d} | 12a_1 \rangle \delta_{1a_1,1a_1},$$

where $\hat{d}$ denotes one of the components (x, y, z) of the dipole operator.

The resulting equations show that the direct contribution is zero, for ionization into both the εa_1 and εe continuum orbitals, due to the monopole overlap. Similarly, symmetry selection rules dictate that the conjugate contribution in the εe case is also zero. The only surviving process is the conjugate contribution in the εa_1 case, but as the monopole overlap decreases rapidly with increasing energy, such processes are expected to contribute significantly only close to threshold. The experimental spectrum was recorded at a photon energy of 614 eV, approximately 320 eV above the C 1s ionization threshold. Hence, the conjugate contribution to the shake-up spectrum would be expected to be negligible. Thus, an alternative mechanism needs to be identified to account for the appearance of the peak associated with the (1,2) ^{2}E satellite states.

Since the I 5p orbitals are involved in the transitions into the (1,2) ^{2}E states, it seems plausible that relativistic effects need to be taken into account. This is not unexpected: the valence shell photoelectron spectrum of CH_3I shows that the $\tilde{X}$ ^{2}E state, due to ionization of the I 5p orbital, is split by spin-orbit interaction into two components separated by ~0.63 eV;[61,62] moreover, the lowest energy transition, n → σ^* (I 5p → σ^*_{CI}), in the UV absorption spectrum is of singlet-triplet type.[63]

When the spin-orbit interaction is taken into consideration, each of the ^{2}E states splits into $E_{1/2}$ and $E_{3/2}$ components, and the 1^2A_1 (C $1s^{-1}$) main state transforms to an $E_{1/2}$ state. Since the Coulomb interaction between the main and shake-up states of the same symmetry ($E_{1/2}$) is possible, the latter states can acquire photoelectron intensity in accord with the ordinary monopole selection rules.

This suggestion, of course, needs to be confirmed by explicit relativistic calculations employing a theoretical method capable of treating the 2h-1p C 1s satellites. Interestingly, the inclusion of spin-orbit coupling proved to be essential in obtaining a satisfactory interpretation of the single and double ionization processes in CH_3I associated with the valence and I 4d orbitals.[64] Alternative, although less likely, mechanisms for the (1,2) ^{2}E states to obtain spectral intensity would be those related to the conjugate part of the photoelectron intensity and to a possible vibronic interaction between the (1,2) ^{2}E and 1^2A_1 states of the pseudo-Jahn-Teller type.[65]

The C 1s photoelectron spectra of CH_3Cl and CH_3Br, which might provide some support for our suggestion that the lowest energy satellite state in the C 1s spectrum of CH_3I acquires intensity through spin-orbit interactions, have not been measured. In CH_4, the lowest energy satellite is located ~17 eV above the main-line.

Proceeding to higher binding energy, the next group of satellites predicted by our calculations is of the C $1s^{-1}$ I 5p → σ^*_{CH} type. The I 5p → σ^*_{CH} electron excitation produces the valence-type singlet and triplet states ($S' = 0,1$) of all possible spatial symmetries (Table III). For the lowest two states, (3,4) ^{2}E, in this group, with vertical ionization energies of 298.90 and 299.31 eV, the σ^*_{CH} orbital is represented by the $13a_1$ orbital, whereas for the higher states, (5,6) ^{2}E, (3,4) $^2A_1$, and (1,2) $^2A_2$, found within the 300.15–300.54 eV interval, the σ^*_{CH} orbital is represented by the 9e orbital. The monopole-allowed (3,4) $^2A_1$ transitions (denoted as B_2 in Fig. 3), with calculated vertical ionization energies of 300.15 and 300.43 eV and relative intensities of 0.0493 and 0.0003, probably contribute to the gradual rise in electron intensity observed around 298 eV.

The main contribution to the maximum occurring at ~297.6 eV in the experimental spectrum is associated with the C $1s^{-1}$ σ_{CI} → σ^*_{CI} (2^2A_1) transition, with a predicted vertical ionization energy of 299.09 eV and a relative photoelectron intensity of 0.8074 (denoted B_1). This satellite state is the lower component ($S' = 1$) in the pair of transitions related to the σ_{CI} → σ^*_{CI} valence excitation.

According to our results, the corresponding $S' = 0$ state, $6\ ^2A_1$ (C $1s^{-1}$ σ_{CI} → σ^*_{CI}), lies at 301.10 eV (denoted C_1) and should be considered as the main source of the spectral intensity ($P = 3.2429$) to the most prominent band in the experimental spectrum, having a maximum at ~300.5 eV. In fact, as can be seen from the data in Table IV, the calculations predict several such states, differing by the admixtures of other configurations. For example, the $8\ ^2A_1$ state (denoted C_2), with a calculated vertical ionization energy of 301.83 eV and a relative spectral intensity of 2.0048, contains an admixture of R′ Rydberg character. The $8\ ^2A_1$ state also contributes to the band observed at 300.5 eV and might be associated with the shoulder occurring around ~301.1 eV. This suggests the presence of

valence-Rydberg mixing resulting from the interaction between the C $1s^{-1}$ $\sigma_{CI} \rightarrow \sigma^*_{CI}$ ($S' = 0$) valence state and the manifold of Rydberg states in which it is embedded.

As mentioned above, our calculations predict a considerable intensity ($P = 0.8074$) for the lowest monopole-allowed C $1s^{-1}$ $\sigma_{CI} \rightarrow \sigma^*_{CI}$ (2^2A_1) satellite transition, which leads to a distinct maximum B_1 in the theoretical spectral envelope. In contrast, the same feature in the experimental spectrum, at ~297.6 eV, has a much smaller relative intensity and is barely visible. The very good agreement between the predicted and observed positions of the band in the spectrum leaves no doubt as to the validity of the present assignment. This raises the question of why the calculated vertical intensity of the B_1 band disagrees so strongly with the experimental data. A possible answer can be given by the obvious analogy between the C $1s^{-1}$ $\sigma_{CI} \rightarrow \sigma^*_{CI}$ ionization and the $\sigma_{CI} \rightarrow \sigma^*_{CI}$ excitation in CH_3I. As is known from the valence electron excitation spectrum, the $\sigma_{CI} \rightarrow \sigma^*_{CI}$ excited state of CH_3I has a repulsive C–I character and leads to the appearance of a broad absorption band.[66,67] The C $1s^{-1}$ $\sigma_{CI} \rightarrow \sigma^*_{CI}$ states can, therefore, also be expected to have dissociative diabatic potential energy surfaces with respect to the C–I separation. Whereas the upper of the states ($S' = 0$) perturbs the manifold of Rydberg states so that states of mixed valence-Rydberg character are formed, the lower state ($S' = 1$) forms the B_1 band characterized by a strongly increased width.

The very satisfactory agreement between the theoretical predictions and the experimental spectrum extends to higher energy. Although the calculated binding energies for some of the features appear slightly higher than those of the corresponding structure evident in the measurement, it seems that the peaks in the theoretical spectrum denoted D, (E_1 and E_2) and (G_1, G_2, and G_3) account for the structure observed around 302, 303–305, and 307–310 eV. Thus, overall, our calculations provide a reliable interpretation of the satellite structure and allow the principal peaks to be assigned. The more detailed information on the nature of states in the high-energy domain of the C $1s^{-1}$ spectrum can be found in Tables IV and S1.

At binding energies above 300 eV the spectrum is dominated by perturbed Rydberg series of the R-type (I $5p^{-1}$). For the states of $^2A_1$ symmetry, the valence C $1s^{-1}$ $\sigma_{CI} \rightarrow \sigma^*_{CI}$ configuration acts as a perturber, as discussed above. As a result, an irregular pattern of excitations, whose energies deviate from those predicted by the Rydberg formula, is observed. Similarly, many Rydberg states of $^2A_2$ and ^2E symmetry are affected by the interaction with valence-type states (Table III) located within the energy range under consideration (Table S1). Above ~304 eV, states with the $(\sigma_{CI})^{-1}$ valence vacancy begin to contribute to the spectrum, and above ~308 eV the $(\sigma_{CH})^{-1}$ Rydberg states (R″) come into play.

The first 3h-2p satellite, associated with the transition to the 11^2A_2 state, is predicted by our calculation at the vertical ionization energy of 303.43 eV. At higher energies the density of 3h-2p states increases.

V. SUMMARY

The C 1s ionization spectrum of CH_3I has been studied both experimentally and theoretically. Photoelectron spectra encompassing the C 1s main-line and the shake-up satellites were recorded at a photon energy of 614 eV with plane polarized synchrotron radiation.

The vertical ionization energies and relative photoelectron intensities were computed using the ADC(4) approximation scheme for the one-particle Green's function which employed also the CVS approximation. In this method, the main 1h transitions, the 2h-1p satellites, and the 3h-2p satellites are treated through fourth, second, and first order of the many-body perturbation theory, respectively. Such a treatment is crucial for a reliable description of the shake-up spectrum. The 6-311++G^{**} basis set was employed in the calculations. The theoretical spectrum agrees qualitatively with the measurements, thereby allowing the main spectral features to be assigned.

The C 1s shake-up satellites of CH_3I can be viewed as valence excitations of the CH_3I core-hole (C $1s^{-1}$) cation. In the nonrelativistic limit, the envelope of the C 1s shake-up spectrum of CH_3I is formed by the 2h-1p ($^2A_1$) transitions which obtain their intensity from configuration interaction with the $^2A_1$ (C $1s^{-1}$) state, represented by the main spectral line.

According to our calculations, two $^2A_1$ shake-up states of the C $1s^{-1}$ $\sigma_{CI} \rightarrow \sigma^*_{CI}$ type and intermediate spins $S' = 0, 1$ play an important role in the spectrum and carry a significant part of the overall intensity. Both C $1s^{-1}$ $\sigma_{CI} \rightarrow \sigma^*_{CI}$ states are expected to be repulsive with respect to the C–I separation. Our calculations show that many of the higher final states resulting from the interaction between the Rydberg states and the upper C $1s^{-1}$ $\sigma_{CI} \rightarrow \sigma^*_{CI}$ ($S' = 0$) valence state have a complex electronic structure. No individual band could be assigned to the $^2A_1$ ($S' = 0$) state as its intensity is redistributed, by the aforementioned interaction, to the affected Rydberg states. In contrast, the $^2A_1$ ($S' = 1$) state forms one of the lowest bands in the spectrum and is characterized by a strongly increased width.

In the nonrelativistic approximation, ^2E and $^2A_2$ states should have no photoelectron intensity for symmetry reasons. However, some of the ^2E states can become visible due to spin-orbit interaction. Our results indicate that the lowest shake-up peak with significant intensity in the experimental spectrum arises from the pair ($S' = 0, 1$) of ^2E (C $1s^{-1}$ I $5p \rightarrow \sigma^*_{CI}$) states. Since here the I 5p orbitals are involved, the spin-orbit interaction should be taken into account. Each of the ^2E states then splits into $E_{1/2}$ and $E_{3/2}$ components, and the $^2A_1$ (C $1s^{-1}$) main state transforms into an $E_{1/2}$ state. Since the Coulomb interaction between the main and shake-up states of the same symmetry ($E_{1/2}$) is possible, the latter states can acquire photoelectron intensities in agreement with the ordinary monopole selection rules. Further experimental and theoretical studies are currently underway to verify this prediction.

Our calculations were performed using a nonrelativistic *ab initio* approach, and no attempt has been made to treat the spin-orbit coupling effect associated with the iodine atom. The present theoretical study should, therefore, be considered as preliminary although allowing many features of the C 1s satellite spectrum of CH_3I to be explained surprisingly well. A more thorough investigation of the spectroscopic implications of spin-orbit coupling represents the subject of our forthcoming publication.

SUPPLEMENTARY MATERIAL

See supplementary material for the full lists of the calculated binding energies and relative photoelectron intensities of the C 1s vertical ionization transitions.

ACKNOWLEDGMENTS

A.B.T. gratefully acknowledges the grant, Grant No. 4.1671.2017/4.6, from the Ministry of Education and Science of the Russian Federation. A.M.B. is grateful to the Favorsky's Institute of Chemistry for a scholarship. R.F. is grateful to the Engineering and Physical Sciences Research Council (EPSRC) for a research studentship. D.M.P.H. was supported by the Science and Technology Facilities Council, United Kingdom. S.T.P. was supported by the U. S. Department of Energy, Office of Science, Office of Basic Energy Sciences, Division of Chemical Sciences, Geosciences, and Biosciences under Contract No. DE-AC02-06CH11357. We are grateful to the SOLEIL staff for running the facility and providing beamtime under Project No. 20150786.

APPENDIX: RECAPITULATION OF THE THEORETICAL RESULTS FOR THE PHOTOIONIZATION CROSS SECTION

The partial photoionization cross section $\sigma_n(\varepsilon)$ related to the final state $|\Psi^N_{n,\varepsilon\lambda}\rangle$ can be expressed as[4,29]

$$\sigma_n(\varepsilon) \propto \sum_{\lambda,v} |D^v_{n,\varepsilon\lambda}|^2. \tag{A1}$$

The transition dipole moment in Eq. (A1) is given by the matrix element,

$$D^v_{n,\varepsilon\lambda} = \langle \Psi^N_{n,\varepsilon\lambda} | \hat{D}_v | \Psi^N_0 \rangle, \tag{A2}$$

of the dipole operator $\hat{D}_v = \sum_i^N \hat{d}_v(i)$ with the components $v = x$, y, z between the N-electron ground state $|\Psi^N_0\rangle$ and the final state $|\Psi^N_{n,\varepsilon\lambda}\rangle$. The latter quantity includes the bound ionic part $|\Psi^{N-1}_n\rangle$ and the continuum free electron part $|\tilde{\varphi}_{\varepsilon\lambda}\rangle$ characterized by the kinetic energy ε and the spatial symmetry λ. For brevity, the index λ is skipped in the notation where unessential.

For the evaluation of the transition dipole moment of Eq. (A2), the final state and the dipole operator are expressed using the formalism of second quantization as $|\Psi^N_{n,\varepsilon}\rangle = c^\dagger_\varepsilon |\Psi^{N-1}_n\rangle$ and $\hat{D}_v = \sum_{pq} d^v_{pq} c^\dagger_p c_q$, where $c^\dagger_p$ and c_q denote, respectively, the creation and destruction operators for the bound orbitals $|\varphi_p\rangle$ and $|\varphi_q\rangle$, while $c^\dagger_\varepsilon$ denotes the creation operator for the continuum orbital $|\tilde{\varphi}_\varepsilon\rangle$ and $d^v_{pq} = \langle \varphi_p | \hat{d}_v | \varphi_q \rangle$. Using these terms, Eq. (A2) can be rewritten as

$$D^v_{n,\varepsilon} = \sum_{pq} d^v_{p,q} \langle \Psi^{N-1}_n | c_\varepsilon c^\dagger_p c_q | \Psi^N_0 \rangle. \tag{A3}$$

Since the continuum orbitals can be expanded in terms of the bound orbitals according to $|\tilde{\varphi}_\varepsilon\rangle = \sum_r |\varphi_r\rangle\langle\varphi_r|\tilde{\varphi}_\varepsilon\rangle$, the second-quantization operator c_ε transforms as[68]

$$c_\varepsilon = \sum_r \langle \tilde{\varphi}_\varepsilon | \varphi_r \rangle c_r. \tag{A4}$$

Inserting Eq. (A4) into Eq. (A3), one obtains

$$D^v_{n,\varepsilon} = \sum_{pqr} d^v_{p,q} s_{\varepsilon,r} \langle \Psi^{N-1}_n | c_r c^\dagger_p c_q | \Psi^N_0 \rangle, \tag{A5}$$

where $s_{\varepsilon,r} = \langle \tilde{\varphi}_\varepsilon | \varphi_r \rangle$ is the overlap matrix element of the continuum and bound orbitals. The $\langle \Psi^{N-1}_n | c_r c^\dagger_p c_q | \Psi^N_0 \rangle$ matrix element can be readily evaluated using the anticommutation relations for the operators of second quantization, and the following equation is obtained:

$$D^v_{n,\varepsilon} = \sum_q d^v_{\varepsilon,q} \langle \Psi^{N-1}_n | c_q | \Psi^N_0 \rangle + \sum_r s_{\varepsilon,r} \langle \Psi^{N-1}_n | \hat{D}_v c_r | \Psi^N_0 \rangle, \tag{A6}$$

where the two terms are referred to as the *direct* and *conjugate* parts, respectively.[17,18,29]

The *direct part*,

$$D^v_{n,\varepsilon\lambda}(\mathrm{I}) = \sum_p d^v_{p,\varepsilon\lambda} \langle \Psi^{N-1}_n | c_p \Psi^N_0 \rangle, \tag{A7}$$

includes the overlaps $x^{(n)}_p = \langle \Psi^{N-1}_n | c_p \Psi^N_0 \rangle$, also referred to as *spectroscopic factors*,[37] which define the probability of finding the final ionic state $|\Psi^{N-1}_n\rangle$ in the pseudo state $|c_p \Psi^N_0\rangle$ produced by the sudden ejection of an electron in the state $|\varphi_p\rangle$ out of the initial state $|\Psi^N_0\rangle$.

In the case of core ionization, the summation in Eq. (A7) reduces to the single term for the specific core orbital k, and the direct part takes on the form

$$D^v_{n,\varepsilon\lambda}(\mathrm{I}) = d^v_{k,\varepsilon\lambda} \langle \Psi^{N-1}_n | c_k \Psi^N_0 \rangle. \tag{A8}$$

If the intensity of the core-hole shake-up process is discussed, the direct part as given by Eq. (A8) can be interpreted as the dipole ionization of a core electron which is accompanied by the monopole excitation of one or more valence electrons. The latter excitation can also be viewed as a reorganization of the electronic structure, taking place in the cationic states $|\Psi^{N-1}_n\rangle$ to provide screening of the initial core hole described by the pseudo state $|c_k \Psi^N_0\rangle$.

The *conjugate part* is given by the expression

$$D^v_{n,\varepsilon\lambda}(\mathrm{II}) = \sum_p s_{p,\varepsilon\lambda} \langle \Psi^{N-1}_n | \hat{D}_v | c_p \Psi^N_0 \rangle, \tag{A9}$$

which for core ionization simplifies to

$$D^v_{n,\varepsilon\lambda}(\mathrm{II}) = s_{k,\varepsilon\lambda} \langle \Psi^{N-1}_n | \hat{D}_v | c_k \Psi^N_0 \rangle. \tag{A10}$$

According to Eq. (A10), in the conjugate shake-up process, the monopole ionization of a core electron is accompanied by the dipole excitation of valence electrons.

According to Eqs. (A8) and (A10), the core ionization cross section can include only the contributions which satisfy specific symmetry conditions. Assuming the applicability of the Abelian subgroup approximation, in the case of the direct part, these conditions are $\Gamma(n) = \Gamma(k)$ and $\Gamma(\lambda) = \Gamma(k) \times \Gamma(v)$, and in the case of the conjugate-part, $\Gamma(\lambda) = \Gamma(k)$ and $\Gamma(n) = \Gamma(k) \times \Gamma(v)$. Since in both cases the second equation is equivalent to the condition $\Gamma(v) = \Gamma(n) \times \Gamma(\lambda)$, the following selection rules can be formulated: (i) For both the direct and the conjugate processes, the overall (electron plus ion) wave function symmetry should match the symmetry of at least one component of the dipole operator. In addition, (ii-a) for the direct part, the ion wave function symmetry should be the same as the symmetry of the main-line process (*monopole selection rule*); and (ii-b) for the conjugate part, the free-electron wave

function symmetry should be the same as the symmetry of the main-line process. Clearly, the selection rules (i) and (ii-b) are not so stringent as it should always be possible to find continuum orbitals of appropriate symmetry which satisfy the conditions.

If the Hartree-Fock (HF) approximation is employed, the ionic states are equivalent to the HF configurations $\left|\Psi_n^{N-1}\right\rangle = \left|\Phi_i^{N-1}\right\rangle$ and $\left|\Psi_n^{N-1}\right\rangle = \left|\Phi_{aij}^{N-1}\right\rangle$ of the h- and 2h-1p-character, respectively. The h-blocks of the direct and conjugate parts then take on the form

$$D_{k,\varepsilon\lambda}^{v}(\mathrm{I}) = d_{k,\varepsilon\lambda}^{v}\left\langle\Phi_i^{N-1}\middle|\Phi_k^{N-1}\right\rangle = \delta_{ik}d_{k,\varepsilon\lambda}^{v}, \tag{A11}$$

$$D_{k,\varepsilon\lambda}^{v}(\mathrm{II}) = s_{k,\varepsilon\lambda}\left\langle\Phi_i^{N-1}\middle|\hat{D}_v\middle|\Phi_k^{N-1}\right\rangle = s_{k,\varepsilon\lambda}\left(\delta_{ik}\sum_r d_{rr}n_r - d_{ki}^{v}\right), \tag{A12}$$

and the 2h-1p-blocks are expressed as

$$D_{aij,\varepsilon\lambda}^{v}(\mathrm{I}) = d_{k,\varepsilon\lambda}^{v}\left\langle\Phi_{aij}^{N-1}\middle|\Phi_k^{N-1}\right\rangle \equiv 0, \tag{A13}$$

$$D_{aij,\varepsilon\lambda}^{v}(\mathrm{II}) = s_{k,\varepsilon\lambda}\left\langle\Phi_{aij}^{N-1}\middle|\hat{D}_v\middle|\Phi_k^{N-1}\right\rangle = s_{k,\varepsilon\lambda}\left(\delta_{jk}d_{ai}^{v} - \delta_{ik}d_{aj}^{v}\right). \tag{A14}$$

In Eqs. (A11)–(A14), the indices i and j denote orbitals which are occupied in the HF ground state and index a denotes unoccupied orbitals. The above results imply that only the conjugate part contributes to the intensity of 2h-1p satellites.

REFERENCES

[1] U. Gelius, J. Electron Spectrosc. Relat. Phenom. **5**, 985 (1974).
[2] H. Siegbahn and L. Karlsson, in *Handbuch der Physik*, edited by W. Mehlhorn (Springer-Verlag, Berlin, 1982), Vol. 31, p. 215.
[3] V. Schmidt, Rep. Prog. Phys. **55**, 1483 (1992).
[4] L. S. Cederbaum, W. Domcke, J. Schirmer, and W. von Niessen, Adv. Chem. Phys. **65**, 115 (1986).
[5] K. Siegbahn, C. Nordling, G. Johansson, J. Hedman, P.-F. Hedén, K. Hamrin, U. Gelius, T. Bergmark, L.-O. Werme, R. Manne, and Y. Baer, *ESCA Applied to Free Molecules* (North Holland, Amsterdam, 1969).
[6] H. M. Köppe, B. S. Itchkawitz, A. L. D. Kilcoyne, J. Feldhaus, B. Kempgens, A. Kivimäki, M. Neeb, and A. M. Bradshaw, Phys. Rev. A **53**, 4120 (1996).
[7] B. Kempgens, A. Kivimäki, H. M. Köppe, M. Neeb, A. M. Bradshaw, and J. Feldhaus, J. Chem. Phys. **107**, 4219 (1997).
[8] B. Kempgens, A. Kivimäki, B. S. Itchkawitz, H. M. Köppe, M. Schmidbauer, M. Neeb, K. Maier, J. Feldhaus, and A. M. Bradshaw, J. Electron Spectrosc. Relat. Phenom. **93**, 39 (1998).
[9] E. E. Rennie, H. M. Köppe, B. Kempgens, U. Hergenhahn, A. Kivimäki, K. Maier, M. Neeb, A. Rüdel, and A. M. Bradshaw, J. Phys. B: At. Mol. Opt. Phys. **32**, 2691 (1999).
[10] E. E. Rennie, B. Kempgens, H. M. Köppe, U. Hergenhahn, J. Feldhaus, B. S. Itchkawitz, A. L. D. Kilcoyne, A. Kivimäki, K. Maier, M. N. Piancastelli, M. Polcik, A. Rüdel, and A. M. Bradshaw, J. Chem. Phys. **113**, 7362 (2000).
[11] K. Kuramoto, M. Ehara, H. Nakatsuji, M. Kitajima, H. Tanaka, A. De Fanis, Y. Tamenori, and K. Ueda, J. Electron Spectrosc. Relat. Phenom. **142**, 253 (2005).
[12] K. Ueda, M. Hoshino, T. Tanaka, M. Kitajima, H. Tanaka, A. De Fanis, Y. Tamenori, M. Ehara, F. Oyagi, K. Kuramoto, and H. Nakatsuji, Phys. Rev. Lett. **94**, 243004 (2005).
[13] R. Sankari, M. Ehara, H. Nakatsuji, A. De Fanis, H. Alsela, S. L. Sorensen, M. N. Piancastelli, E. Kukk, and K. Ueda, Chem. Phys. Lett. **422**, 51 (2006).
[14] M. Ehara, H. Nakatsuji, M. Matsumoto, T. Hatamoto, X.-J. Liu, T. Lischke, G. Prümper, T. Tanaka, C. Makochekanwa, M. Hoshino, H. Tanaka, J. R. Harries, Y. Tamenori, and K. Ueda, J. Chem. Phys. **124**, 124311 (2006).
[15] M. Ehara, K. Kuramoto, H. Nakatsuji, M. Hoshino, T. Tanaka, M. Kitajima, H. Tanaka, A. De Fanis, Y. Tamenori, and K. Ueda, J. Chem. Phys. **125**, 114304 (2006).
[16] T. Gejo, M. Machida, K. Honma, E. Shigemasa, E. Nakamura, N. Kosugi, and Y. Tamenori, J. Electron Spectrosc. Relat. Phenom. **156**, 274 (2007).
[17] J. Berkowitz, J. L. Dehmer, Y.-K. Kim, and J. P. Desclaux, J. Chem. Phys. **61**, 2556 (1974).
[18] R. L. Martin and D. A. Shirley, J. Chem. Phys. **64**, 3685 (1976).
[19] U. Becker and D. A. Shirley, Phys. Scr. **T31**, 56 (1990).
[20] A. D. O. Bawagan and E. R. Davidson, Adv. Chem. Phys. **110**, 215 (1999).
[21] T. Åberg, Phys. Rev. **156**, 35 (1967).
[22] A. Reimer, J. Schirmer, J. Feldhaus, A. M. Bradshaw, U. Becker, H. G. Kerkhoff, B. Langer, D. Szostak, R. Wehlitz, and W. Braun, Phys. Rev. Lett. **57**, 1707 (1986).
[23] L. J. Medhurst, T. A. Ferrett, P. A. Heimann, D. W. Lindle, S. H. Liu, and D. A. Shirley, J. Chem. Phys. **89**, 6096 (1988).
[24] L. J. Medhurst, P. A. Heimann, M. R. F. Siggel, D. A. Shirley, C. T. Chen, Y. Ma, S. Modesti, and F. Sette, Chem. Phys. Lett. **193**, 493 (1992).
[25] K. J. Randall, A. L. D. Kilcoyne, H. M. Köppe, J. Feldhaus, A. M. Bradshaw, J.-E. Rubensson, W. Eberhardt, Z. Xu, P. D. Johnson, and Y. Ma, Phys. Rev. Lett. **71**, 1156 (1993).
[26] T. Reich, P. A. Heimann, B. L. Petersen, E. Hudson, Z. Hussain, and D. A. Shirley, Phys. Rev. A **49**, 4570 (1994).
[27] O. Hemmers, S. B. Whitfield, N. Berrah, B. Langer, R. Wehlitz, and U. Becker, J. Phys. B: At. Mol. Opt. Phys. **28**, L693 (1995).
[28] H. M. Köppe, A. L. D. Kilcoyne, J. Feldhaus, and A. M. Bradshaw, J. Electron Spectrosc. Relat. Phenom. **75**, 97 (1995).
[29] J. Schirmer, G. Angonoa, and L. S. Cederbaum, Z. Phys. D **5**, 253 (1987).
[30] G. Angonoa, O. Walter, and J. Schirmer, J. Chem. Phys. **87**, 6789 (1987).
[31] A. Lisini, G. Fronzoni, and P. Decleva, J. Phys. B: At. Mol. Opt. Phys. **21**, 3653 (1988).
[32] J. Schirmer, M. Braunstein, and V. McKoy, Phys. Rev. A **44**, 5762 (1991).
[33] H. Nakatsuji, Chem. Phys. Lett. **177**, 331 (1991).
[34] G. Bandarage and R. R. Lucchese, Phys. Rev. A **47**, 1989 (1993).
[35] G. Fronzoni, G. De Alti, and P. Decleva, J. Phys. B: At. Mol. Opt. Phys. **32**, 5357 (1999).
[36] A. Thiel, J. Schirmer, and H. Köppel, J. Chem. Phys. **119**, 2088 (2003).
[37] J. Schirmer, L. S. Cederbaum, and O. Walter, Phys. Rev. A **28**, 1237 (1983).
[38] J. Schirmer and G. Angonoa, J. Chem. Phys. **91**, 1754 (1989).
[39] I. Powis, D. M. P. Holland, E. Antonsson, M. Patanen, C. Nicolas, C. Miron, M. Schneider, D. Yu. Soshnikov, A. Dreuw, and A. B. Trofimov, J. Chem. Phys. **143**, 144304 (2015).
[40] R. Forbes, A. De Fanis, C. Bomme, D. Rolles, S. T. Pratt, I. Powis, N. A. Besley, S. Nandi, A. R. Milosavljević, C. Nicolas, J. D. Bozek, J. G. Underwood, and D. M. P. Holland, J. Chem. Phys. **149**, 094304 (2018).
[41] R. Forbes, A. De Fanis, C. Bomme, D. Rolles, S. T. Pratt, I. Powis, N. A. Besley, M. Simon, S. Nandi, A. R. Milosavljević, C. Nicolas, J. D. Bozek, J. G. Underwood, and D. M. P. Holland, J. Chem. Phys. **149**, 144302 (2018).
[42] P. Baltzer, L. Karlsson, M. Lundqvist, and B. Wannberg, Rev. Sci. Instrum. **64**, 2179 (1993).
[43] J. Jauhiainen, A. Ausmees, A. Kivimäki, S. J. Osborne, A. Naves de Brito, S. Aksela, S. Svensson, and H. Aksela, J. Electron Spectrosc. Relat. Phenom. **69**, 181 (1994).
[44] A. P. Hitchcock and C. E. Brion, J. Electron Spectrosc. Relat. Phenom. **13**, 193 (1978).
[45] L. S. Cederbaum, W. Domcke, and J. Schirmer, Phys. Rev. A **22**, 206 (1980).
[46] N. V. Dobrodey, A. I. Streltsov, and L. S. Cederbaum, Phys. Rev. A **65**, 023203 (2002).
[47] N. V. Dobrodey, A. I. Streltsov, L. S. Cederbaum, C. Villani, and F. Tarantelli, J. Chem. Phys. **117**, 3533 (2002).
[48] N. V. Dobrodey, A. I. Streltsov, L. S. Cederbaum, C. Villani, and F. Tarantelli, Phys. Rev. B **66**, 165103 (2002).
[49] A. I. Streltsov, N. V. Dobrodey, and L. S. Cederbaum, J. Chem. Phys. **119**, 3051 (2003).

[50] N. V. Kryzhevoi, R. Santra, and L. S. Cederbaum, J. Chem. Phys. **135**, 084302 (2011).
[51] O. Plekan, V. Feyer, R. Richter, A. Moise, M. Coreno, K. C. Prince, I. L. Zaytseva, T. E. Moskovskaya, D. Yu. Soshnikov, and A. B. Trofimov, J. Phys. Chem. A **116**, 5653 (2012).
[52] The ADC(4) code originally written by G. Angonoa, O. Walter and J. Schirmer; further developed by N. V. Dobrodey and A. B. Trofimov.
[53] M. W. Schmidt, K. K. Baldridge, J. A. Boatz, S. T. Elbert, M. S. Gordon, J. H. Jensen, S. Koseki, N. Matsunaga, K. A. Nguyen, S. Su, T. L. Windus, M. Dupuis, and J. A. Montgomery, J. Comput. Chem. **14**, 1347 (1993).
[54] M. S. Gordon and M. W. Schmidt, in *Advances in Electronic Structure Theory: GAMESS a Decade Later*, edited by C. E. Dykstra, G. Frenking, K. S. Kim, and G. E. Scuseria (Elsevier, Amsterdam, 2005), p. 1167.
[55] R. Krishnan, J. S. Binkley, R. Seeger, and J. A. Pople, J. Chem. Phys. **72**, 650 (1980).
[56] T. Clark, J. Chandrasekhar, G. W. Spitznagel, and P. V. R. Schleyer, J. Comput. Chem. **4**, 294 (1983).
[57] M. N. Glukhovtsev, A. Pross, M. P. McGrath, and L. Radom, J. Chem. Phys. **103**, 1878 (1995).
[58] M. J. Frisch, G. W. Trucks, H. B. Schlegel, G. E. Scuseria, M. A. Robb, J. R. Cheeseman, G. Scalmani, V. Barone, B. Mennucci, G. A. Petersson, H. Nakatsuji, M. Caricato, X. Li, H. P. Hratchian, A. F. Izmaylov, J. Bloino, G. Zheng, J. L. Sonnenberg, M. Hada, M. Ehara, K. Toyota, R. Fukuda, J. Hasegawa, M. Ishida, T. Nakajima, Y. Honda, O. Kitao, H. Nakai, T. Vreven, J. A. Montgomery, Jr., J. E. Peralta, F. Ogliaro, M. Bearpark, J. J. Heyd, E. Brothers, K. N. Kudin, V. N. Staroverov, T. Keith, R. Kobayashi, J. Normand, K. Raghavachari, A. Rendell, J. C. Burant, S. S. Iyengar, J. Tomasi, M. Cossi, N. Rega, J. M. Millam, M. Klene, J. E. Knox, J. B. Cross, V. Bakken, C. Adamo, J. Jaramillo, R. Gomperts, R. E. Stratmann, O. Yazyev, A. J. Austin, R. Cammi, C. Pomelli, J. W. Ochterski, R. L. Martin, K. Morokuma, V. G. Zakrzewski, G. A. Voth, P. Salvador, J. J. Dannenberg, S. Dapprich, A. D. Daniels, O. Farkas, J. B. Foresman, J. V. Ortiz, J. Cioslowski, and D. J. Fox, GAUSSIAN 09, Revision C.01, Gaussian, Inc., Wallingford, CT, 2010.
[59] *Structure of Free Polyatomic Molecules—Basic Data*, edited by K. Kuchitsu (Springer, Berlin, 1998).
[60] R. S. Mulliken, J. Chem. Phys. **23**, 1833 (1955).
[61] L. Karlsson, R. Jadrny, L. Mattsson, F. T. Chau, and K. Siegbahn, Phys. Scr. **16**, 225 (1977).
[62] D. M. P. Holland, I. Powis, G. Öhrwall, L. Karlsson, and W. von Niessen, Chem. Phys. **326**, 535 (2006).
[63] R. Locht, B. Leyh, H. W. Jochims, and H. Baumgärtel, Chem. Phys. **365**, 109 (2009).
[64] M. Pernpointer, J. P. Zobel, E. Fasshauer, and A. N. Sil, Chem. Phys. **407**, 39 (2012).
[65] H. Köppel, W. Domcke, and L. S. Cederbaum, Adv. Chem. Phys. **57**, 59 (1984).
[66] S. Eden, P. Limão-Vieira, S. V. Hoffmann, and N. J. Mason, Chem. Phys. **331**, 232 (2007).
[67] A. Fahr, A. K. Nayak, and M. Kurylo, Chem. Phys. **197**, 195 (1995).
[68] J. Schirmer, *Many-Body Methods for Atoms, Molecules and Clusters* (Springer, International Publishing, 2018).